

Finite Element Analysis of a Mooring Chain Link

Abhijit Venkat (22110008), Hari Balaji (22110092), Jayeeta Kol

IIT Gandhinagar

Under Prof. Sushobhan Sen

1. Introduction

Moorings are engineered assemblies that secure seaborne vessels to fixed points—such as quays, buoys or anchors—to prevent unwanted drift under wind, current and wave action [6]. The flexible link between the vessel and its anchoring point is provided by mooring chains, which must sustain large static and dynamic loads without failure. In practice one distinguishes between studded and studless chain designs; in this work we focus exclusively on studless chains, whose simpler geometry facilitates both manufacture and inspection but whose curved link profiles demand careful stress-analysis to avoid local overstress.

Studless mooring chains are ubiquitous in offshore operations, from oil-and-gas platforms to commercial shipping terminals. Accurately predicting their load-bearing capacity under complex service conditions is therefore critical to ensure both safety and regulatory compliance. A detailed finite-element analysis allows engineers to identify regions of peak stress and displacement, verify compliance with applicable standards (e.g. DNV or ISO chain specifications), and optimize link geometry or material selection for specific operational scenarios.

In our study, the geometry of a single chain link was created and discretized in Gmsh, taking care to capture the curved shank and bearing surfaces with sufficiently fine mesh control in high-stress regions. The resulting mesh was imported into PrePoMax, which interfaces directly with the open-source CalculiX solver to perform the three-dimensional static analysis. Material behaviour was assumed linear-elastic (Grade 40 steel), and boundary conditions were prescribed so as to replicate typical chain installation: one end of the link is fixed, while a uniaxial tensile load is applied to the opposite end.

The primary objective of this project is twofold:

1. Determine the spatial distribution of von Mises stress in the loaded link.
2. Quantify the maximum nodal displacements in all three coordinate directions and finding out the maximum displacement.

2. Geometry



Figure 1. Mooring Chain [5]

The above image represents a mooring chain. For our analysis, we modeled a single chain link in Gmsh, with half-links on

either side as shown in the figures below:

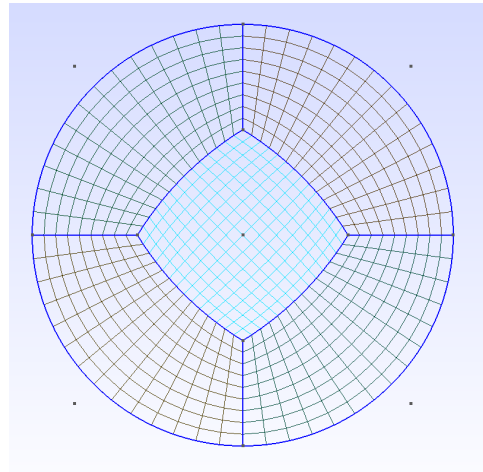


Figure 2. Mesh Cross-Section

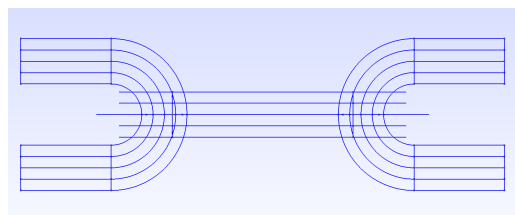


Figure 3. Chain link geometry (top-view)

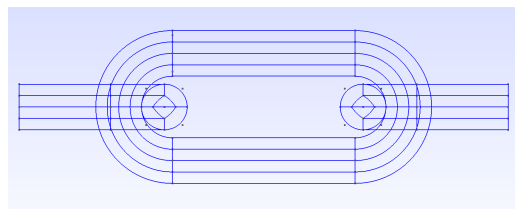


Figure 4. Chain link geometry (side-view)

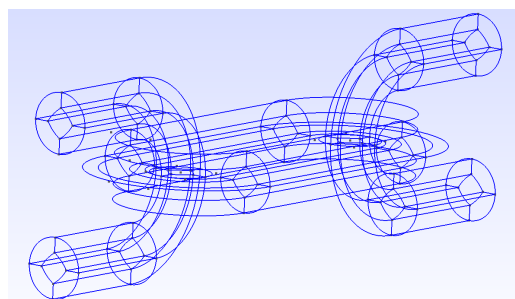


Figure 5. Complete Mesh Wireframe

The dimensions of the model are listed in the figure below:

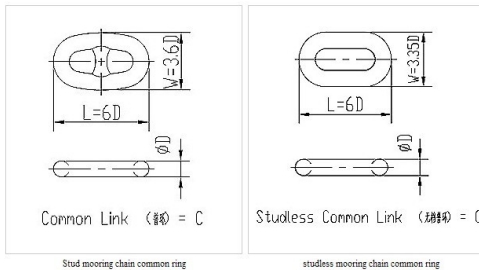


Figure 6. Mooring Chain Dimensions [4]

We selected a diameter of $D = 100$ mm for the chain, and so consequently the length of the chain came out to be $L = 600$ mm and the width came out to be $W = 335$ mm.

3. Meshing

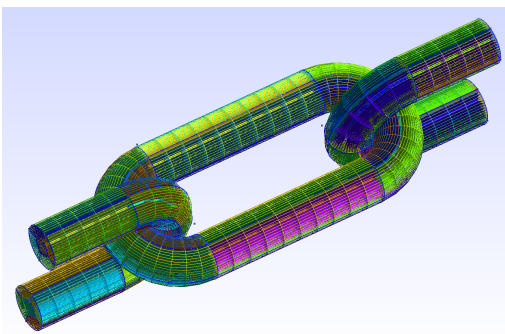


Figure 7. Meshed Geometry

The above figure shows the meshed geometry of the chain. To make the mesh, the following process was followed:

- A circle of diameter 100 mm was created.
- A bulged square was created in the centre of the circle, and its vertices were connected to the edges of the circle dividing it into five sections.
- The edges were made into transfinite curves and the circle was meshed.
- The circular mesh was extruded into the shape of the chain link using the translate and rotate functions, and the half-link was also done in the same way.

Also, a mesh independence study was conducted. Three different mesh sizes were chosen. The statistics of the three meshes are shown below:

Refinement Level	Number of Nodes	Number of Quadrangles	Number of Hexahedra
0	9666	5976	8640
1	68704	22950	64800
2	168386	42336	161280
3	308770	64792	297920

Table 1. Mesh Statistics

4. Constitutive Properties and Constraints

Constitutive Properties

The type of chain we chose was *Grade R4*, and the material of choice is high grade steel. The material properties chosen are listed as follows:

Material Property	Value
Density	7800 kg/m ³
Young's Modulus	210 GPa
Poisson's Ratio	0.3

Table 2. Constitutive Properties

Constraints and Boundary Conditions

For solving the problem, it was necessary to give certain constraints to the solver in PrePoMax. First, the necessary surfaces in contact were defined, along with the surfaces which represented the ends of the chain.

One end is fixed, and the other end is loaded. These were the boundary conditions given:

- **Fixed End:** Fixed ($u(0) = 0$)
- **Loaded End:** Uniform Pressure

For the interaction between the half-links and the full link, a *hard* contact condition with a friction coefficient of 0.1 was used.

This condition ensures transmission of compressive stresses between the surfaces in contact, and does not permanently enforce a rigid connection like the *tied* condition.

5. Results and Discussions

The simulation was run for all the three meshes for different loads. Reference values for the Grade R4 chain are shown below [3]:

- **Chain Diameter:** 100 mm
- **Studless Proof Load:** 6912 kN
- **Breaking Load:** 9864 kN

To apply the uniform pressure boundary condition, we divide the force by the cross sectional area:

$$P = \frac{F}{A_{cs}}$$

$$A_{cs} = \pi R_{cs}^2$$

Since $R_{cs} = 50$ mm = 0.05 m and there are two such cross-sections, we get the value of the uniform pressure to be:

$$P = 440.0316 \text{ MPa}$$

Refinement Level	Max. von Mises Stress (MPa)	Max. x-disp. (mm)	Max. y-disp. (mm)	Max. z-disp. (mm)	Max. Total Disp. (mm)
0	3960	2.615	6.761	6.631	9.413
1	3670	3.278	8.325	1.399	1.628
2	3660	3.311	8.406	1.423	1.653
3	3697	3.326	8.438	0.0269	1.665

Table 3. Von Mises Stress and Displacements in Three Dimensions for the Studless Proof Load

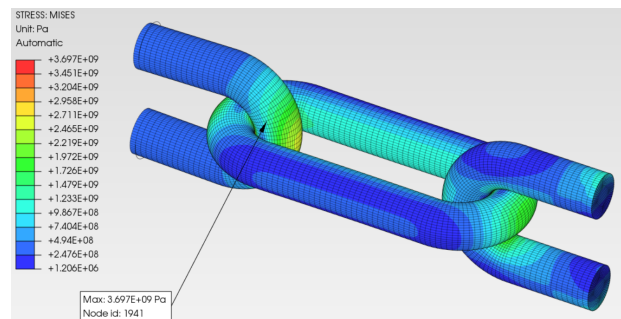


Figure 11. Refinement Level 3

Von Mises Stress Contours

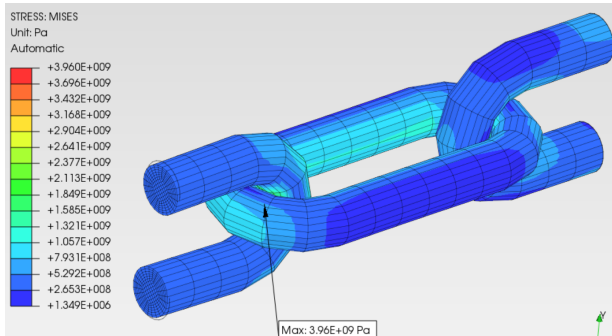


Figure 8. Refinement Level 0

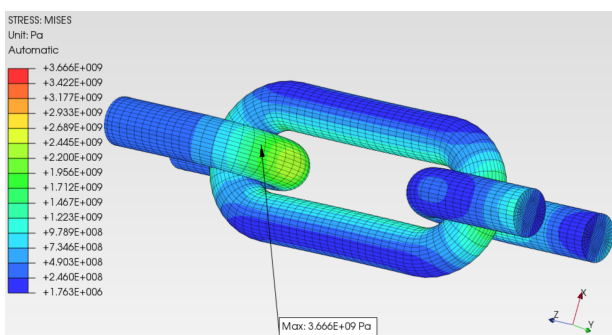


Figure 9. Refinement Level 1

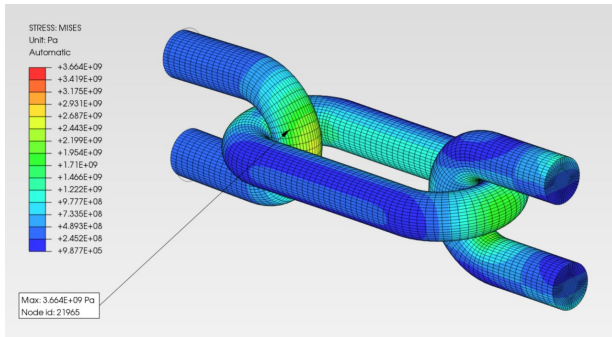


Figure 10. Refinement Level 2

As seen from the contour plots of the von Mises stress distribution, a clear pattern can be observed. Firstly, as refinement is increased, a green-yellow-red contour transition can be seen near the contact points, indicating higher von Mises stress in these locations. Also, the values seem to converge to a value of $\sigma_{vonMises} \approx 3700\text{ MPa}$.

Total Displacement Contours

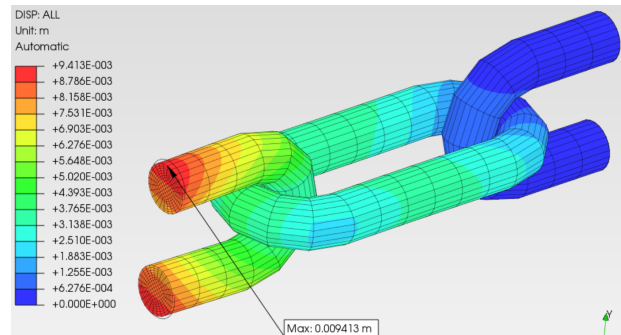


Figure 12. Refinement Level 0

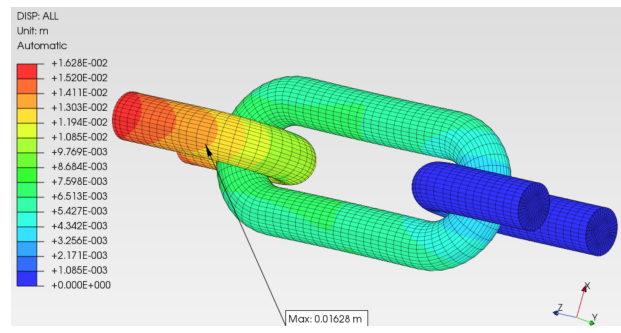


Figure 13. Refinement Level 1

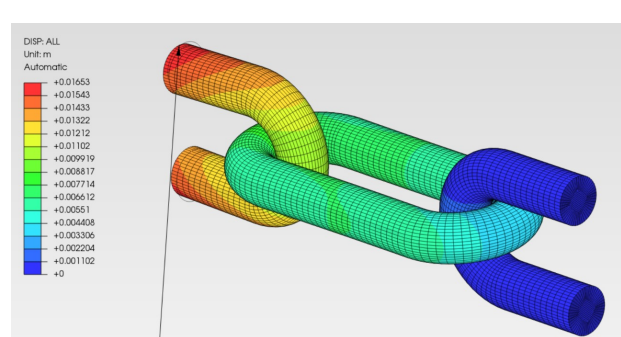


Figure 14. Refinement Level 2

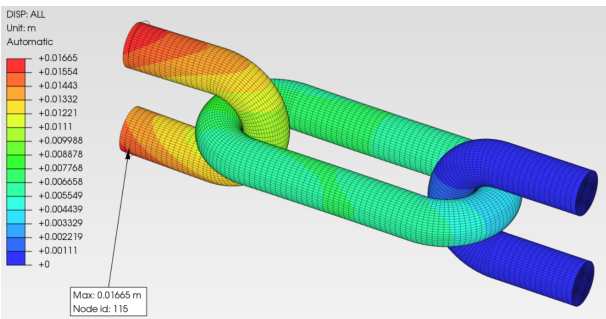


Figure 15. Refinement Level 3

A similar trend can be observed in the displacement contours. According to our boundary conditions, one of the ends is fixed. This is reflected in the contour plots as the blue contour near one end. In the region near the fixed boundary condition, the displacements are quite low. On the other end, where the uniform load is applied, we can see relatively heavy deformation and deviation from the original configuration. Similar to the von Mises trend, the maximum displacement also seems to converge as the refinement is increased. Nowhere in these contour plots do we encounter non-physical values, thus solidifying our approach towards this problem.

6. Convergence

Two parameters were used to determine if convergence has been achieved, mainly, the maximum von Mises stress (σ) and the maximum total displacement (d). We obtained the values of these parameters for each level of refinement and obtained the following plots.

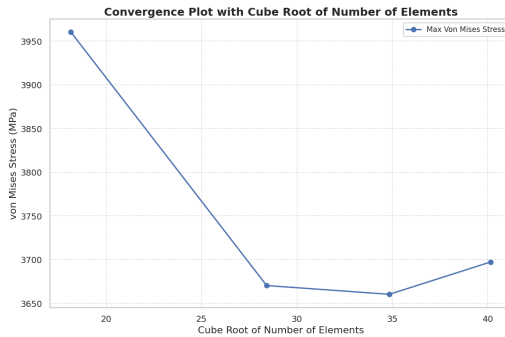


Figure 16. Max von Mises stress v/s cube root of number of elements

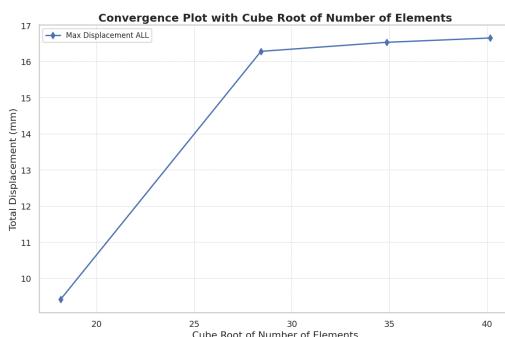


Figure 17. Max displacement v/s cube root of number of elements

Figure 16 and Figure 17 show the maximum von Mises stress and maximum total displacement, respectively, plotted

against the cube-root of the total number of elements, $N^{1/3}$. We observe the following:

- Apparent Convergence:** For the medium-fidelity meshes (approximately $N = 2.3 \times 10^4$ to 4.2×10^4 elements), both the stress and displacement curves begin to flatten, indicating that the solution is approaching a mesh-independent limit.
- Deviation at Finest Mesh:** Upon further refinement to $N = 6.5 \times 10^4$, however, the computed maxima *deviate* slightly from the trend. Instead of remaining on the plateau, both quantities move “away” from their apparent limits.
- Interpretation:** Such non-monotonic behavior at the finest grid level suggests that mesh *quality*, rather than sheer element count, is governing accuracy. In particular, poorly-shaped elements can introduce spurious interpolation and integration errors that *outweigh* the benefits of added resolution.

Mesh Quality Metrics. The following parameters are critical in assessing whether a given triangulation will produce reliable results under refinement:

- **Aspect Ratio**, $\frac{\ell_{\max}}{\ell_{\min}}$: High aspect-ratio (“needle”) triangles amplify interpolation error.
- **Skewness**: Deviation from the ideal element shape (e.g. equilateral). High skewness degrades gradient accuracy.
- **Non-Orthogonality**: Angle between face normal and edge vector. Large non-orthogonality introduces cross-diffusion errors in flux integrals.
- **Jacobian/Warpage**: Measures distortion in the mapping from reference to physical element. Negative Jacobians indicate inverted elements and must be avoided.
- **Size Grading**: The ratio of adjacent element sizes, typically kept below 1.2. Abrupt changes break the error-cancellation properties of the numerical scheme.

Recommendations for True Mesh Independence.

1. Enforce *upper bounds* on aspect ratio and skewness during mesh generation.
2. Apply local refinement only where $\nabla\sigma$ or ∇u are large, rather than a uniform global increase (In our case, increase refinement near the contact points).
3. Control size gradation to ensure smooth transitions ($\leq 1.2\times$ growth per element).

With these practices in place, the medium-fidelity mesh already lies within the mesh-independent regime, and further increases in element count will yield *consistent* (and *monotonic*) approach to the true solution without the risk of degradation caused by poor element shapes.

7. Validation

For validation, we considered a simple axially loaded member of the same diameter as that of the chain. Similar to the calculations in section 5, we get the stress to be about 440 MPa.

The yield strength of high-strength steel used in the manufacture of mooring chains is equal to about 580 MPa [1]. As long as the von Mises stress is lower than the Yield strength of the material, it hasn't undergone plastic deformation and can regain its original shape. As we can see from the contour plots, the von Mises stress magnitude is lower at the parallel bars, which can be compared to our analogous axial force member. This stress is lower than the Yield Strength, and therefore, the material hasn't yielded in these locations.

As far as the contact regions are concerned, it would be very difficult to find an analytical solution for their von Mises stress or their deformation. But we can say for sure that these locations (contact points) are the weak points and would be the first regions to undergo yielding. As we can also see from the von-Mises contour plots, the contact regions are the ones under very high stresses, even being greater than the yield strength of steel itself. In summary:

- Parallel bars of full chain link - von Mises stress < yield strength
- Contact regions - von Mises stress > yield strength

AI disclosure

We used ChatGPT minimally to paraphrase some sentences in our report and also to help us extract important information from the references cited below.

8. Acknowledgements

We would like to thank Prof. Sushobhan Sen for teaching us the principles that enabled us to successfully complete this project. His expertise and insights were invaluable.

We would also like to thank the TAs Chirag Nagar and Ankita Singh for their assistance with our project. We could not have completed the project had they not solve our problems.

Lastly, we would like to thank IIT Gandhinagar for providing us with the platform and opportunity to do this project.

References

- [1] Sotra Anchor & Chain AS, *Chain mechanical properties*, Accessed: 2025-04-23, Aug. 2021. [Online]. Available: <https://www.sotra.net/wp-content/uploads/2021/08/CHAIN-MECHANICAL-PROPERTIES.pdf>.
- [2] Dennis M. Kochmann, ETH Zurich, *Introduction to finite element analysis*, Accessed: 2025-04-23, 2025. [Online]. Available: https://ethz.ch/content/dam/ethz/special-interest/mavt/mechanical-systems/mm-dam/documents/Notes/IntroToFEA_red.pdf.
- [3] Pilotfits Engineering, *Offshore mooring chain*, <https://pilotfits.com/products/mooring-chain/>, Accessed: 2025-04-19, 2025.
- [4] Hi-Sea Marine, *Grade r4 mooring chain*, <https://en.hisamarine.com/products/grade-r4-mooring-chain.html>, Accessed: 2025-04-19, 2025.
- [5] Titan Marine Products, *G43 long link mooring chain*, <https://titanmarineproducts.com/product/long-link-mooring-chain/>, Accessed: 2025-04-19, 2025.
- [6] Wikipedia contributors, *Mooring*, <https://en.wikipedia.org/wiki/Mooring>, Accessed: 2025-04-19, 2025.